Freeform Optics for Achieving Collimated and Uniform Light Distribution in LCD-Type UV-Curable 3D Printing

Zhengbo Zhu

***Abstract*—Ultraviolet light (UV)-curable three dimensional (3D) printing has emerged as a prominent additive manufacturing technology, finding diverse applications in industries such as figurine production, artifact restoration, dentistry, jewelry design, and etc. For liquid crystal display (LCD) type UV-curable 3D printers, achieving a uniform and collimated light distribution of the illumination system holds paramount importance, as it directly influences printing precision. This study proposes a novel light tailoring method employing freeform lenses to attain high efficient illumination system for 3D printers. The proposed illumination system mainly comprises a high-power UV LED, a freeform lens, and a Fresnel lenses. Initially, a ray mapping between the source domain and the target domain is established to design the preliminary freeform lens, assuming a point-like light source. Subsequently, considering the physical dimension of the high-power UV LED, the preliminary lens is further optimized to generate a uniform illuminance distribution in a rectangular shape. Finally, a Fresnel lens is employed to collimate the light. The results demonstrate a full width half maximum of the angular distribution of less than $\pm 5°$, indicating a narrow spread of the light beam. The illuminance distribution within the specified domain exhibits an impressive level of uniformity, exceeding 90%.**

***Index Terms*—Freeform optics design, illumination optics, UV-curable 3D printing.**

I. Introduction

THREE-DIMENSIONAL (3D) printing techniques, commonly referred to as the rapid prototyping, have undergone significant advancements in the past two decades and have found extensive utilization across various fields [1]. Among the diverse range of 3D printing technologies, ultraviolet light (UV)-curable 3D printing emerges as a prominently employed rapid prototyping process owing to its notable advantages such as swift printing speed, high precision, low energy consumption, and eco-friendliness. Specifically, the UV-curable 3D printing, founded on the principle of selectively solidifying photosensitive resin using UV light under digital signal control, facilitates the incremental accumulation of resin layers to construct 3D objects. Over the years, numerous UV-curing mechanisms have been developed, mainly including SLA, DLP, and LCD-based 3D printing technologies [2], [3], [4], [5]. The SLA-type 3D printer utilizes a UV laser as the light source, enabling precise control over the scanning cross-section profile via the rotation of a mirror. This process allows for the curing of one layer at a time, followed by the sequential curing of subsequent layers, resulting in the superimposition of layers to form a 3D object. On the other hand, the DLP-type 3D printer employs a UV projector as the light source and manipulates the projected light using a digital micromirror element. This technology enables the projection of one layer at a time, followed by the complete curing of that specific layer before moving on to the next. In contrast, LCD-type 3D printers achieve rapid solidification by selectively rendering transparent areas on an LCD panel. This approach offers advantages such as lower cost and faster printing speeds compared to SLA and DLP printers. However, the lifespan of LCD-type 3D printers is limited due to the inherent damage caused by exposure to UV light. The operational principle of an LCD-type 3D printer involves a computer program that transmits image signals to an LCD, generating specific transparent regions through which UV light can pass and expose the UV curable resin within the resin vat. Following the curing of each layer, the platform elevates to replenish the resin, subsequently descending to expose and cure the resin through UV light. This process enables the gradual solidification and fabrication of intricate 3D objects in a step-by-step manner. The working principle of the LCD-type 3D printer is illustrated in Fig. 1.

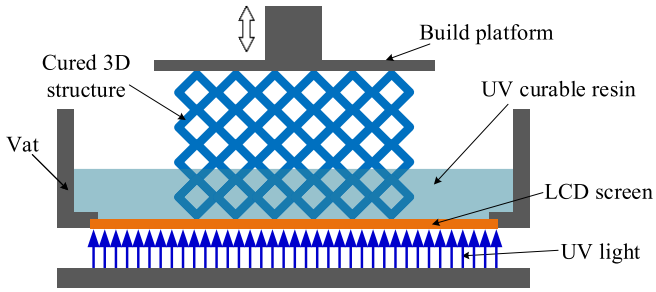

Fig. 1. Schematic diagram of LCD-type 3D printer.

In LCD-type 3D printing systems, achieving a uniform and collimated light distribution on the LCD is crucial as it directly affects the precision of 3D shaping. The energy density of the

Manuscript received 15 May 2023; revised 23 June 2023; accepted 9 July 2023. Date of publication 12 July 2023; date of current version 25 July 2023. This work was supported in part by the National Natural Science Foundation of China under Grant 62205116, in part by the Postdoctoral Innovative Research Project of Hubei Province in 2022, and in part by China Postdoctoral Science Foundation under Grant 2022M711244.

The author is with the School of Optical and Electronic Information, Huazhong University of Science and Technology, Wuhan, Hubei 430074, China (e-mail: zhuzb2015@163.com).

Digital Object Identifier 10.1109/JPHOT.2023.3294478

illumination influences the 3D printing speed. Some research and explorations have been conducted for a higher light performance of LCD-type 3D printers. For instance, a commercially available LCD- type 3D printer (Phrozen, Shuffle XL-2019 [6]) utilized UV LEDs with a lens array optical module to generate collimated light distribution. However, this approach results in dim regions at the intersections of the lens array, leading to a decline in critical dimension uniformity and the accuracy of printed objects. To address this issue, Lin et al. implemented a diffuser film, two crossed brightness enhancement films, and a privacy filter on the LED array, enabling the achievement of a uniform and quasi-collimated light distribution. As a result, the uniformity of the illuminance distribution reached 80%, with an angular distribution of less than $\pm 15°$ [7].

In this study, freeform optics is employed to tackle the design challenges associated with the illumination system in LCD-type 3D printers. A freeform surface refers to a surface that lacks translational or rotational symmetry about axes normal to the mean plane. It provides higher design freedom and spatial flexibility compared with traditional surfaces, making it suitable for various applications in imaging optics and non-imaging optics [8], [9], [10], [11], [12]. A high-power UV LED with a large emitting area is chosen as the light source. The goal is to create a compact freeform lens to regulate the light distribution from the selected light source, resulting in a uniform light spot that matches the size of the LCD. The design process begins by establishing a ray mapping between the source domain and the target domain to develop the initial freeform lens, assuming a point-like light source. Subsequently, considering the actual dimensions of the UV LED, the initial lens needs to be further optimized to achieve a uniform illuminance distribution within the desired lighting area. To collimate the light beam, a Fresnel lens is utilized. Finally, the effectiveness of the proposed optical solution is verified via simulation and experimentation.

The comprehensive design process, which integrates the problem statement and the freeform optics design, is thoroughly explained in Section II. In Section III, a series of design examples are provided to demonstrate the feasibility of the proposed method. This section also includes a discussion of the limitations of the proposed method. Finally, the work is concluded in Section IV.

II. Design Methodology

The proposed configuration of the illumination system for LCD-type 3D printers, which mainly incorporates a freeform lens, a high-power UV LED, and a Fresnel lens, is illustrated in Fig. 2. The function of the freeform lens is to control the light emitted by the UV LED, with the objective of achieving a uniform illuminance distribution in a rectangle shape. On the other hand, the Fresnel lens is positioned in close proximity to the LCD panel, with its flat side facing the LED source and the threaded side facing the LCD. It acts as a collimating element without altering the energy distribution on the LCD.

To achieve optimal collimation of the divergent light beam using the Fresnel lens, it is crucial to design the freeform lens within a limited volume. However, high-power LEDs typically have larger luminous areas, directly impacting the size of the freeform lens. This poses a significant challenge in efficiently controlling light from the extended light source while meeting the lighting requirements [14], [15], [16], [17], [18], [19], [20], [21], [22], [23]. There have been mainly three approaches to address this challenge including optimization method, feedback method and simultaneous multiple surfaces (SMS) method [17]. The optimization method involves representing the freeform surfaces using basis functions and optimizing their coefficients to minimize the deviation between the actual lighting effect and the desired one [18], [19], [20]. The feedback method is an iterative process that uses the differences between the actual illumination and the desired one to update the target illumination via a feedback function [21]. The SMS method constructs multiple surfaces to couple edge wavefronts from the corners of the extended LED source [22], [23].

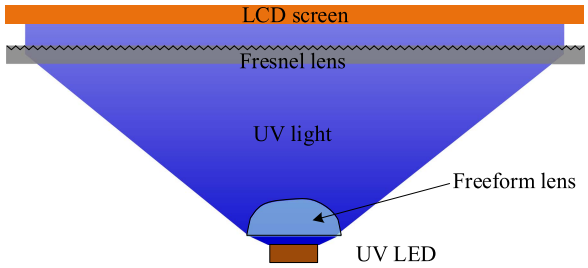

Fig. 2. Geometrical layout of the proposed illumination system for LCD-type UV-curable 3D printer.

In this study, a two-step process is taken for designing a compact freeform lens producing a uniform light distribution with an extended UV LED source. Initially, with a point-like source assumption, the ray mapping method is employed to conduct the preliminary lens design. Subsequently, considering the physical dimension of the high-power UV LED, the initial lens is optimized using the localized surface control method [14] to improve the optical performance.

A. Initial Freeform Lens Design

In the field of optics design, the importance of a well-designed initial structure cannot be overstated, as it significantly contributes to the success of the subsequent optimization processes. Extensive research has been conducted on designing freeform illumination optics with point-like source assumption where the source size is negligible compared with the freeform optics [17]. Here, the ray mapping method is selected to design the initial freeform lens for its flexible ability and relative simplicity compared with the other choices. This method is adopted by solving a source-target map **m** between the source domain and the target domain satisfying the flux conversion and the boundary condition, then, constructing the freeform surface to realize the computed source-target map **m**. Fig. 3 illustrates the principle of the ray mapping method, where the freeform optics is used to transfer the energy from the source domain S to the target domain T in a prescribed way.

In the process of energy transfer, energy conservation and boundary condition should be followed, which are constrained

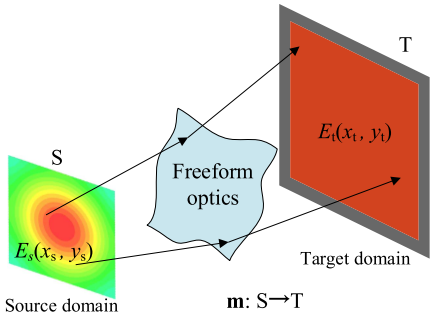

Fig. 3. Ray mapping principle.

as:

$$\det(\nabla \mathbf{m}(x_s, y_s)) = \frac{E_s(x_s, y_s)}{E_t(\mathbf{m}(x_s, y_s))}, (x_s, y_s) \in \mathrm{S} \quad (1)$$

$$\mathbf{m}(\partial \mathrm{S}) = \partial \mathrm{T}. \quad (2)$$

Equation (1) ensures the energy conservation for an infinitesimal light tube, where Es and Et are the energy distribution in the source domain S and the target domain T, respectively, $\nabla \mathbf{m}$ represents the Jacobi matrix of map $\mathbf{m}$. Equation (2) makes the boundary of the source domain map to the boundary of the target domain, where ∂S and ∂T denote the boundaries of the source and the target. The map $\mathbf{m}$ can be solved by the optimal transport method [24], [25], and the freeform surface can be constructed based on the obtained map $\mathbf{m}$ [26]. However, the calculated map $\mathbf{m}$ might not yield an integrable surface normal field $\mathbf{N}$ in complex lighting configurations, which means that the calculated surface cannot redirect the rays to the desired position on the target. So, the normal field $\mathbf{N}$ should satisfy the integrability condition [27], which can be expressed as:

$$\mathbf{N} \cdot (\nabla \times \mathbf{N}) = 0. \quad (3)$$

The normal field $\mathbf{N}$ can be calculated via the law of Snell's reflection with the information of the incident rays and the corresponding outgoing rays, which are determined by the source-target map $\mathbf{m}$. Next, an iterative process is implemented to change the integrable target map to satisfy the energy conservation (1) and boundary condition (2). At the end of the iteration, (1)–(3) can be simultaneously satisfied. The pseudo-code of the initial freeform lens design with point-like source assumption is shown in Algorithm 1.

The detailed method of deriving integrable mapping can be found in Refs. [24], [25].

B. Compact Freeform Lens Optimization

Here, the example is aimed to redirect rays from a LED source to form a uniform light distribution with a rectangle boundary. The light distance (distance between the LED and the illumination target) is set as 120 mm, and the light pattern size is 160 mm × 120 mm. The freeform lens is designed with the point-like source assumption detailed above. The size of the obtained freeform lens is about 28 mm × 24 mm × 14 mm (length, width and height). The illuminance distribution results are shown in Fig. 4. It can be found from the result that the

Algorithm 1: Initial Freeform Lens Design.

IMPUT: incident ray parameters **i**, desired illumination size $a \times b$, distance between LED and target plane H, distance between LED and lens h, lens's refractive index n.
OUTPUT: initial freeform surface (x, y, z)

```
function IFLD (i, a, b)
  compute initial map m0 with (i, a, b, H, h, n)
  construct initial freeform surface (x0, y0, z0) with m0
  while (Δi < Δi+1)
    trace rays and obtain the real target map t'
    calculate deviation Δi between predefined target map t and the real target map t'
    update predefined target map t while satisfying (1) and (2)
    generate new source-target map m
    construct freeform surface (xi+1, yi+1, zi+1) with m
    i = i+1
  end while
  return (x, y, z)
end function
```

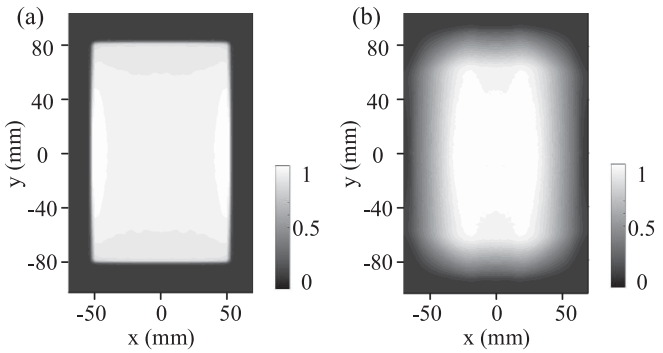

Fig. 4. Illuminance distributions of the freeform lens with (a) a point-like source with 0.1 mm × 0.1 mm luminous area, and (b) an actual LED source with 6 mm × 6 mm luminous area.

ray mapping method demonstrates an accurate light control for a point-like LED source. However, when a LED with larger luminous area is employed, the light distribution deteriorates, resulting in a light pattern characterized by a bright center and dark edges. So, it is imperative to optimize the initial freeform lens for extended LED sources.

For light sources with Lambertian radiation properties, such as LEDs, the illuminance value of a check point on the target plane is directly determined by the localized surface where the light beam passes through [28]. Any change in the curvature of the localized surface will result in corresponding variations in the illuminance value of that check point. So, for the freeform surface optimization, there are two problems need to be addressed: (1) identifying the localized freeform surface that is traversed by the light beam, thereby contributing to the illuminance of the check point on the target plane; and (2) developing a surface modification strategy to optimize the localized freeform surface

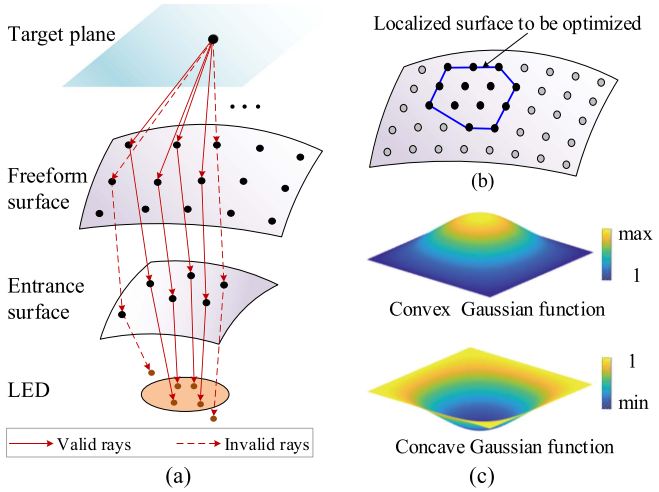

Fig. 5. Schematic of the freeform surface optimization: (a) Backward ray-tracing to find the localized surface; (b) the obtained localized freeform surface; (c) two functions for the localized surface optimization.

Algorithm 2: Freeform surface optimization

IMPUT: initial freeform surface (x_0, y_0, z_0), LED source S_{LED}
OUTPUT: optimized freeform surface (x, y, z)
function FSO(x_0, y_0, z_0, S_{LED})
  while ($U_i < U_{i+1}$ & $\eta_{i+1} > \eta_{min\_th}$)
    calculate illuminance on the target plane [14]
    evaluate U and η
    get the check point with max or min illuminance
    backward ray-tracing, get the localized surface $(x_{loc}, y_{loc}, z_{loc})$
    optimize the localized surface with Gaussian function
    obtain new freeform surface (x_i, y_i, z_i)
    $i = i+1$
  end while
  return (x, y, z)
end function

for achieving a desired illumination when using an extended LED source.

As shown in Fig. 5(a), a backward ray-tracing approach is utilized to trace the rays from a check point on the target plane to the freeform surface, the entrance surface and the LED in sequence. Only if the ray falls inside the LED's luminous area, the traced ray is valid and relevant to the effective area of the freeform surface to the check point. The freeform surface is described as a finite number of sampled points, and the entrance surface of the lens is an analytical one. For a given check point, the rays from this point are traced to all independent points on the freeform surface. The normal vector field of the freeform surface can be numerically calculated by the finite difference scheme. Consequently, the intersecting points on the entrance surface and the LED luminous area can be calculated analytically. This backward ray-tracing process can be formulated as a matrix manipulation, allowing for an efficient calculation in MATLAB. The intersection points of the valid rays with the freeform surface are collected to determine the localized surface that requires modification, as depicted by the blue box in Fig. 5(b).

Here, a convex Gaussian function and a concave Gaussian function are employed, shown in Fig. 5(c), to change the curvature distribution of the localized freeform surface. The convex Gaussian function has the ability to converge light, thus making the corresponding illuminance of the check point increase, while the concave Gaussian function diverges the light beam, and makes the corresponding illuminance of the check point decrease. When the illuminance value of the check point is lower than the desired value, a convex function is applied to modify the corresponding localized surface. Conversely, if the illuminance value is higher than the desired value, the concave function is considered. In the optimization process, the illuminance uniformity and the energy utilization should be considered at the same time. Here, illuminance uniformity U is quantified as the ratio of the minimum illuminance to the maximum illuminance within the effective lighting area, while energy utilization η is quantified as the ratio of the energy received within the effective lighting area to the LED emission energy. The pseudo-code of the freeform lens optimization is shown in Algorithm 2.

The more detailed implement of the localized freeform surface optimization process can be found in our previous work [14].

III. Design Examples and Discussion

In this section, some design examples are provided to verify the effectiveness of the proposed method. The borosilicate glass with a refractive index of 1.47 is chosen as the material of the freeform lens considering its excellent temperature resistance. A high-power UV LED customized by Bytech Electronics Co., Ltd [29] is selected as the light source. It has a central wavelength of 405 nm and a luminous area measuring 12.84 mm × 12.84 mm. The entrance surface of the freeform lens is chosen as flat for the convenience of manufacturing and installing. A 13-inch LCD panel with an aspect ratio of 16:10 is selected. The dimension of its working area is about 294 mm × 166 mm. The distance between the LED and the LCD is set 180 mm according to the application demand. The Fresnel lens with a focal length of 180 mm is used to collimate the light. If all the light from the LED is collected, the lens size becomes infinite. Therefore, the maximum collection angle of the LED is chosen as 82° for a compact lens structure. In the following design examples, the size of the freeform lens is controlled by adjusting the distance between the LED and the entrance surface of the freeform lens.

The distance between the LED and the entrance surface of the lens h is set 5 mm, 6 mm, 7 mm and 8 mm, respectively. For each configuration, the design process introduced in Section II is implemented to obtain the initial freeform lens and the optimized freeform lens in sequence, then, the optical performance analysis is conducted based on Monte-Carlo ray tracing in LightTools [30]. In the freeform surface optimization process for the extended LED source, the minimum energy utilization η_{min_th} is set 0.5. The design results are shown in Fig. 6.

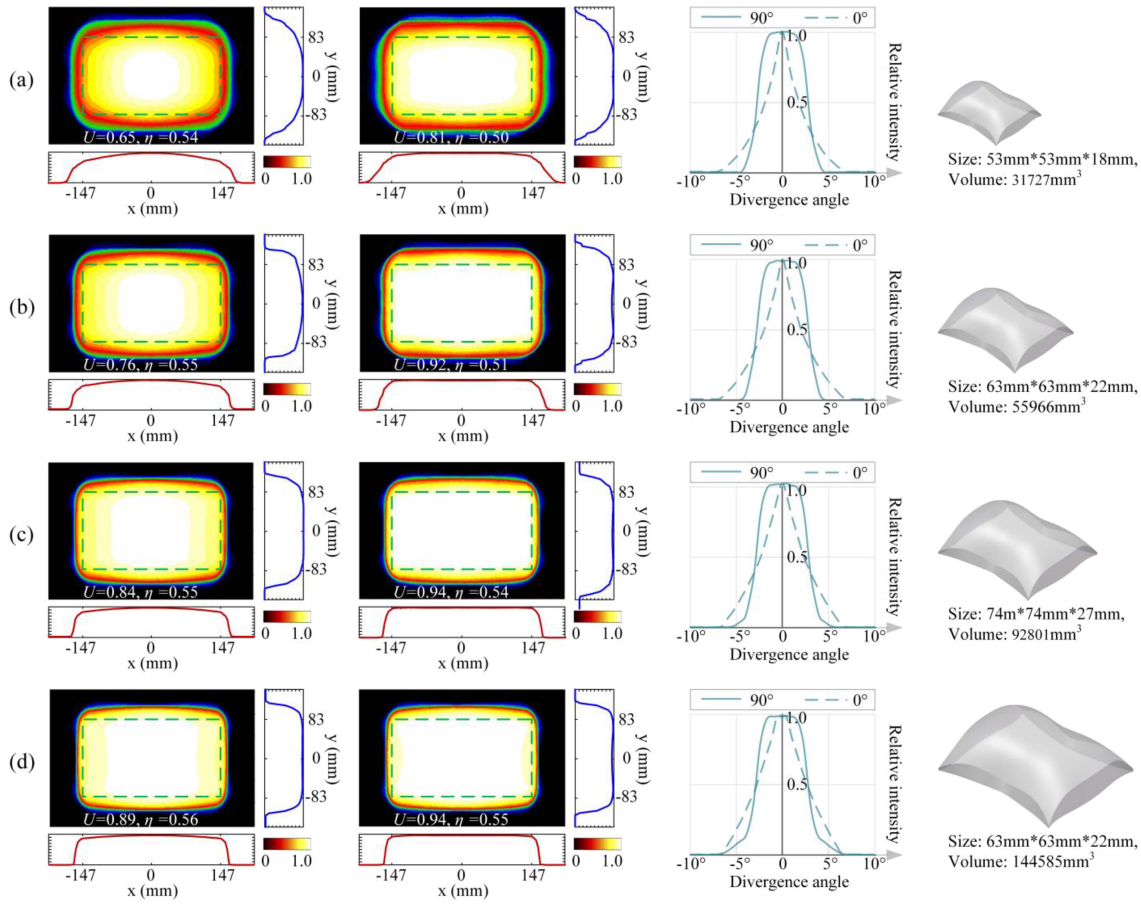

Fig. 6. Design results for different configurations distinguished by the distance between the LED and the entrance surface of the freeform lens h: (a) $h = 5$ mm; (b) $h = 6$ mm; (c) $h = 7$ mm and (d) $h = 8$ mm. From left to right, the columns depict the following information: The illuminance distribution generated by the initial freeform lens on the LCD, the illuminance distribution generated by the optimized freeform lens on the LCD, the light beam divergence property after passing through the fresnel lens, the optimized freeform lens model.

The illuminance distributions presented in Fig. 6 are measured using a detector placed behind the Fresnel lens. The effective illumination area, representing the LCD working area, is denoted by the green dotted line box. The third column of Fig. 6 illustrates the divergence angle of the light beam in two orthogonal directions. Due to factors such as the large luminous area, non-negligible volume of the freeform lens, and spherical aberration of the Fresnel lens, the divergence angle in the orthogonal direction is not completely identical. It can be found from these results that: (1) The optimization of the initial freeform lens has a remarkable effect on improving light uniformity U. (2) The optimization leads a decrease in energy utilization η. This is mainly because that when the illuminance value of the illumination boundary is raised, it inevitably causes more energy overflow outside the effective lighting area. (3) Increasing the distance h between the LED and the lens enhances the light uniformity of the LCD. However, this leads to a significant increase in the volume of the freeform lens, posing great challenges in terms of manufacturing and material costs. (4) The collimation of the light beam decreases as the volume of lens increase, which is manifested in an increase in light intensity beyond the angle space of $\pm 5°$ when the freeform lens volume increase.

Then, a prototype of the second design (the distance between the LED and the entrance surface of the lens h is 6 mm) is implemented, as shown in Fig. 7(a). The freeform lens is fabricated by the compression molding method with an accuracy of ± 100 μm. The Fresnel lens with an equal tooth width and a focal length of 180 mm is set at 180 mm from the UV LED. To visualize the light distribution generated by the freeform lens on the LCD, an A3 paper is used as a substitute for the LCD, and the lighting effect on the A3 paper is recorded using a camera, as depicted in Fig. 7(c). It is important to note that stray light is blocked using a black pyramid in the optical system. The upper part of the blocker has an opening size consistent with the LCD size, while the lower part is connected to the boundary of the freeform lens. This arrangement accounts for the sharp boundary observed in the light pattern.

As a rule of thumb, the illuminance distribution is assessed by the 9-points method with UV light tester LS125+UVALED-X3 [32]. The detector of the UV light tester is placed on the Fresnel lens to conduct the illuminance test (now, the A3 paper is removed). To minimize the testing error, three sets of lenses and UV LEDs are selected for the experimental tests. The results are listed in Table I, showing a high level of consistency among the three experimental groups. However, analysis of the data reveals

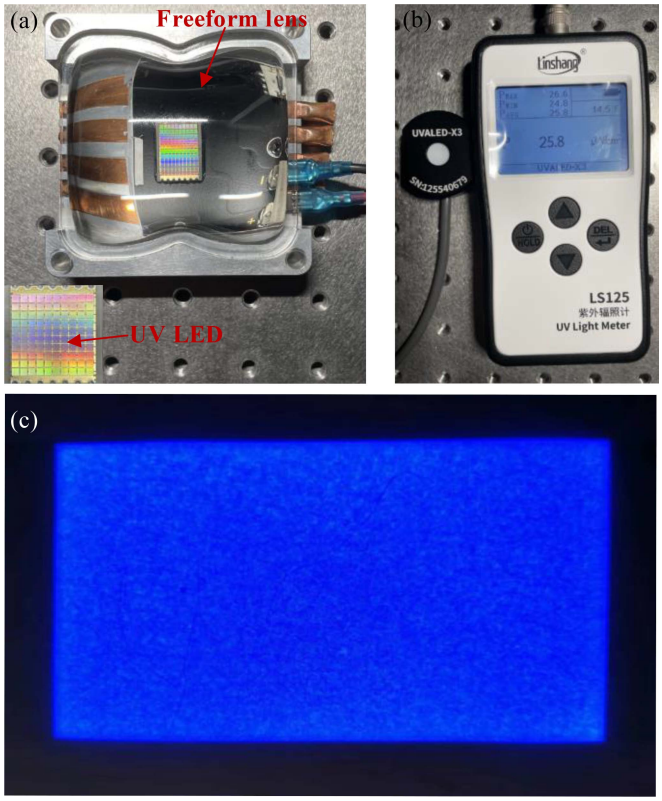

Fig. 7. Experimental verification of the second design: (a) The prototypes of the freeform lens and UV LED; (b) UV light tester LS125+UVALED-X3 [32]; (c) the recorded light pattern.

TABLE I
RECORDED DATA BY UV LIGHT TESTER

Test group	Recorded data (μW/cm²)			U
# 1	12627	13501	13080	0.9080
	12708	13403	13283	
	13301	13228	13907	
# 2	12887	13627	13435	0.9008
	12975	13526	13478	
	13704	13754	14306	
# 3	13569	14142	14056	0.9044
	13725	14114	13675	
	14048	14210	15003	

a disparity between the actual illumination and the simulation one. This deviation in performance can be attributed to various sources of error, such as the fabrication error of the freeform lens, the discrepancy between the actual radiation properties of the utilized UV LED and the ideal Lambertian radiation property. By displacing the A3 paper along the axis to record the position of the light pattern edge, the measured light angular space aligns closely with the simulation value.

To assess the effectiveness of the proposed illumination system, a UV-curable 3D printer incorporating two distinct light modules is utilized: the proposed light module and a commercial light module employing UV LEDs equipped with a lens array.

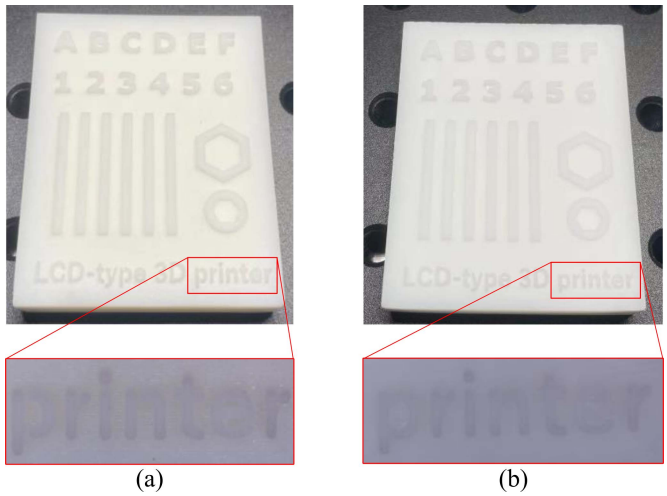

Fig. 8. Photographs of the printed 3D objects by (a) the commercial light module and (b) the proposed light module.

TABLE II
MEASURED DIMENSION OF THE PRINTED 3D OBJECTS

Test group	Average width (μm)		
Proposed light module	213	205	195
Commercial light module	235	187	215

The central part of the LCD is selected for printing the 3D objects. The photographs of the printed 3D objects can be found in Fig. 8. Upon close examination of the magnified images, notable discrepancies between the two objects become apparent: (1) The surface of the 3D object printed using the light module proposed in this work exhibits a smoother texture compared to the one printed using the commercial light module. (2) The small-sized structure produced with the commercial light source displays evident flaws, particularly noticeable as discontinuities in the letters "p" and "r." These differences can be attributed to two factors: the uniformity of the illuminance distribution on the LCD panel and the collimation of the light beam emitted from the LCD.

Furthermore, to ascertain the consistency of the printing performance across various locations on the LCD, three linear objects measuring 200 μm in width are printed at three distinct positions: the top left corner of the LCD, the center of the LCD, and the midpoint between these two locations. The dimensional characteristics of these objects are analyzed using a microscope to evaluate the lateral accuracy and size variation. The results, listed in Table II, indicate that the size deviation of objects printed using the commercial light module is greater compared to those printed using the proposed light module. This discrepancy can be attributed to the inherent challenge of ensuring uniform illumination performance across each LED source and sub-lens, thereby leading to variations in light distribution on the LCD.

The implementation of a lighting system utilizing a single freeform lens demonstrates efficacy when applied to the LCD panels with relatively small sizes. However, as the dimensions of

the LCD panel increase, there arises a necessity to augment the LED power in order to maintain the desired 3D molding speed. However, this augmentation in LED size will inevitably result in a substantial enlargement of the freeform lens dimensions. The precision manufacturing of large freeform lenses at a low cost presents a notable challenge. Besides, the freeform lens with large size is incompatible with the compact and lightweight structure that is desired for 3D printers. In this case, it is crucial to explore alternative forms of lighting solutions, such as the solution described in Ref. [7]. In the proposed lighting system, if the lighting uniformity is blindly pursued, it will inevitably lead to the decline of energy utilization. So, it is imperative to make a compromise between better illuminance uniformity and high energy utilization.

IV. Conclusion

This work has developed a freeform illumination system for achieving collimated and uniform light distribution in LCD-type UV-curable 3D printing. The design process is divided in two steps: designing the initial freeform lens with the point-like source assumption for a relatively acceptable optical performance, and optimizing the initial lens to achieve uniform illuminance distribution while maintaining a high energy utilization within the desired lighting area on the LCD screen. The Fresnel lens is employed to collimate the light from the freeform lens. The effectiveness of the proposed method is verified by multiple design examples incorporating simulations and experimental tests. The lighting solution proposed in this work might hold significant potential for optimizing UV-Curable 3D printers with relatively small sizes of LCDs.

Acknowledgment

Zhengbo Zhu thanks Shili Wei for his valuable help in establishing the ray mapping method for the initial freeform lens design.

References

[1] N. Shahrubudin, T. C. Lee, and R. Ramlan, "An overview on 3D printing technology: Technological, materials, and applications," *Procedia Manuf.*, vol. 35, pp. 1286–1296, 2019.
[2] E. O. Olakanmi, R. F. Cochrane, and K. W. Dalgarno, "A review on selective laser sintering/melting (SLS/SLM) of aluminium alloy powders: Processing, microstructure, and properties," *Prog. Mater. Sci.*, vol. 74, pp. 401–477, 2015.
[3] B. Utela et al., "A review of process development steps for new material systems in three dimensional printing (3DP)," *J. Manuf. Process.*, vol. 10, pp. 96–104, 2008.
[4] P. Parandoush and D. Lin, "A review on additive manufacturing of polymer-fiber composites," *Composite Struct.*, vol. 182, pp. 36–53, 2017.
[5] A. J. Capel et al., "3D printing for chemical, pharmaceutical and biological applications," *Nature Rev. Chem.*, vol. 2, no. 12, pp. 422–436, 2018.
[6] Jun. 2023. [Online]. Available: http://www.mastech3d.com
[7] D. Z. Lin et al., "Development of a quasi-collimated UV LED backlight for producing uniform and smooth 3D printing objects," *Opt. Exp.*, vol. 30, no. 9, pp. 14759–14769, 2022.
[8] A. A. Mingazov et al., "On the use of the supporting quadric method in the problem of designing double freeform surfaces for collimated beam shaping," *Opt. Exp.*, vol. 28, no. 15, pp. 22642–22657, 2020.
[9] K. Desnijder, P. Hanselaer, and Y. Meuret, "Freeform Fresnel lenses with a low number of discontinuities for tailored illumination applications," *Opt. Exp.*, vol. 28, no. 17, pp. 24489–24500, 2020.
[10] S. Babadi, R. Ramirez-Iniguez, T. Boutaleb, and T. Mallick, "Performance comparison of a freeform lens and a CDTIRO when combined with an LED," *IEEE Photon. J.*, vol. 9, no. 5, Oct. 2017, Art. no. 6501008.
[11] K. Falaggis et al., "Freeform optics: Introduction," *Opt. Exp.*, vol. 30, no. 4, pp. 6450–6455, 2022.
[12] Y. Ning et al., "Freeform surface graded optimization of deformable mirrors in integrated zoom and image stabilization system through vectorial ray tracing and image point freezing method," *IEEE Photon. J.*, vol. 12, no. 1, Feb. 2020, Art. no. 6900316.
[13] S. Wei et al., "Compact freeform illumination optics design by deblurring the response of extended sources," *Opt. Lett.*, vol. 46, no. 11, pp. 2770–2773, 2021.
[14] Z. Zhu et al., "Freeform illumination optics design for extended LED sources through a localized surface control method," *Opt. Exp.*, vol. 30, no. 7, pp. 11524–11535, 2022.
[15] Z. Ding et al., "Direct design of thin and high-quality direct-lit LED backlight systems," *IEEE Photon. J.*, vol. 13, no. 2, Apr. 2021, Art. no. 8200210.
[16] D. Wu, K. Wang, and V. G. Chigrinov, "Feedback reversing design method for uniform illumination in LED backlighting with extended source," *J. Display Technol.*, vol. 10, no. 1, pp. 43–48, 2013.
[17] R. Wu et al., "Design of freeform illumination optics," *Laser Photon. Rev.*, vol. 12, no. 7, 2018, Art. no. 1700310.
[18] E. V. Byzov et al., "Optimization method for designing double-surface refractive optical elements for an extended light source," *Opt. Exp.*, vol. 28, no. 17, pp. 24431–24443, 2020.
[19] Z. Zhu, S. Wei, Z. Fan, Y. Yan, and D. Ma, "Design ultra-compact aspherical lenses for extended sources using particle swarm optical optimization algorithm," *IEEE Photon. J.*, vol. 11, no. 6, Dec. 2019, Art. no. 8201614.
[20] X. Mao et al., "Fast design method of smooth freeform lens with an arbitrary aperture for collimated beam shaping," *Appl. Opt.*, vol. 58, no. 10, pp. 2512–2521, 2019.
[21] L. Hongtao et al., "A fast feedback method to design easy-molding freeform optical system with uniform illuminance and high light control efficiency," *Opt. Exp.*, vol. 21, no. 1, pp. 1258–1269, 2013.
[22] S. Sorgato et al., "Design of illumination optics with extended sources based on wavefront tailoring," *Optica*, vol. 6, no. 8, pp. 966–971, 2019.
[23] P. Benı´ tez et al., "Simultaneous multiple surface optical design method in three dimensions," *Opt. Eng.*, vol. 43, no. 7, pp. 1489–1502, 2004.
[24] S. L. Wei et al., "Least-squares ray mapping method for freeform illumination optics design," *Opt. Exp.*, vol. 28, no. 3, pp. 3811–3822, 2020.
[25] Z. Zhu et al., "Freeform illumination optics for 3D targets through a virtual irradiance transport," *Opt. Exp.*, vol. 29, no. 10, pp. 15382–15392, 2021.
[26] Z. Feng, B. D. Froese, and R. Liang, "Freeform illumination optics construction following an optimal transport map," *Appl. Opt.*, vol. 55, no. 16, pp. 4301–4306, 2016.
[27] F. R. Fournier, W. J. Cassarly, and J. P. Rolland, "Fast freeform reflector generation using source-target maps," *Opt. Exp.*, vol. 18, no. 5, pp. 5295–5304, 2010.
[28] W. R. McCluney, *Introduction to Radiometry and Photometry*. Norwood, MA, USA: Artech House, 2014.
[29] Jun. 2023. [Online]. Available: http://www.zsbytech.com
[30] Jun. 2023. [Online]. Available: https://www.synopsys.com/optical-solutions/lighttools.html
[31] Jun. 2023. [Online]. Available: https://www.linshangtech.cn